Inorganic Chemistry

Forum Article

pubs.acs.org/IC

Imaging DNA with Fluorochrome Bearing Metals

Hoonsung Cho,[†] Yanyan Guo,[†] David E. Sosnovik,[‡,§] and Lee Josephson*[,†,‡]

[†]Center for Translational Nuclear Medicine and Molecular Imaging, [‡]Martinos Center for Biomedical Imaging, Department of Radiology, and [§]Cardiovascular Research Center, Cardiology Division, Massachusetts General Hospital, Harvard Medical School, Boston, Massachusetts 02114, United States

ABSTRACT: Molecules that fluoresce upon binding DNA are widely used in assaying and visualizing DNA in cells and tissues. However, using light to visualize DNA in animals is limited by the attenuation of light transmission by biological tissues. Moreover, it is now clear that DNA is an important mediator of dead cell clearance, coagulation reactions, and an immunogen in autoimmune lupus. Attaching metals (e.g., superparamagnetic nanoparticles, gadolinium ions, radioactive metal ions) to DNA-binding fluorochromes provides a way of imaging DNA in whole animals, and potentially humans, without light. Imaging metal-bearing, DNA-binding fluorochromes and their target DNA by magnetic resonance imaging may shed light on the many key roles of DNA in health and disease beyond the storage of genetic information.

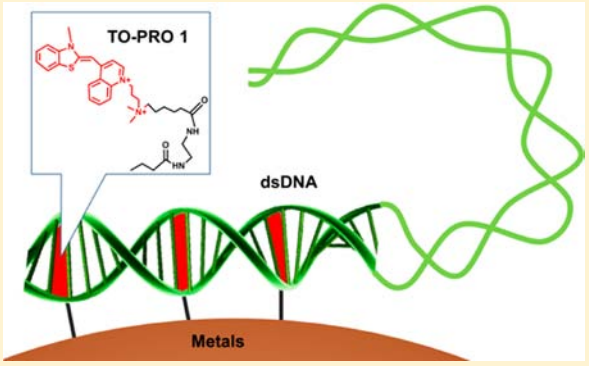

INTRODUCTION

Molecules that fluoresce upon binding DNA are widely used in polymerase chain reaction (PCR) assays and in visualization of DNA in cells and tissues. However, the fluorescence of DNA-binding molecules cannot be used to image DNA in small or large animals because of tissue light attenuation. Moreover, it is now clear that DNA plays many important roles in biology and disease, other than its nuclear role in genetic information storage. The limitations of fluorescence, together with DNA's many important extracellular roles in disease, reviewed below, suggest the need for methods of DNA detection that might be applied to whole body imaging.

We therefore describe the use of DNA-binding fluorochromes as targeting vehicles for metals, metals that allow DNA imaging by whole-body-imaging modalities by magnetic resonance imaging (MRI), and, potentially, by single-photon emission computerized tomography (SPECT) or positron emission tomography (PET). (By "metals", we mean the metallic elements used as cations or metal oxides.) These "metal-bearing" fluorochromes retain their ability to fluorescence upon binding DNA, while being detectable through the presence of their metal by a whole-body-imaging modality.

Our chemistry involves the synthesis of the NHS ester of the DNA-binding fluorochrome TO-PRO 1, "TO-PRO 1 NHS", which can be attached to magnetic nanoparticles (NP) or gadolinium chelates, as shown in Figure 1.[1,2] The fluorochrome-functionalized nanoparticle obtained, "FFNP", consists of 10 TO-PRO 1 species attached to a Feraheme (FH) nanoparticle (NP). FFNP forms FFNP/DNA microaggregates with PCR-generated DNA, which can be detected as changes in T_2, the spin−spin relaxation time of protons. FFNP has also been used to image the DNA of tumors induced into necrosis (plasma membrane permeability) by chemotherapeutic agents. TO-PRO 1 (TO) has also been attached to a gadolinium chelate, yielding Gd-TO, a DNA-binding gadolinium chelate that has been used to image the DNA of cardiomyocytes induced into necrosis by sustained ischemia.[3,4]

Before discussing the use of fluorochrome metals described in Figure 1 for imaging DNA, we briefly review some of the nongenetic roles of DNA in biological systems, which provide an impetus for the development of whole-body-imaging DNA techniques.

NONGENETIC ROLES OF DNA

DNA-Mediated Clearance of Dead and Dying Cells. After cell necrosis, DNA is a mediator of macrophage infiltration and dead cell clearance.[5] A lack of DNase II, an enzyme that degrades DNA in lysosomes, causes the accumulation of fragmented DNA in macrophages, activating *TNFα* and *IFNβ* gene expressions and innate immune response.[6,7] Dead and dying microbes and host cells also release DNA, which is a potent antigen and proinflammatory molecule.[8,9] A failure to clear the DNA of apoptotic and dying cells may play a role in the generation of anti-DNA antibodies, which are a hallmark of systemic lupus erythematosus (SLE).

DNA and Coagulation. DNA is a component of neutrophil extracellular traps, which play a role in linking infection, inflammation, and deep vein thrombosis.[10−12] Hence, DNase, already used for treating cystic fibrosis, might be an effective thrombolytic therapy.[13]

Special Issue: Metals in Medicine and Health

Received: February 15, 2013
Published: May 6, 2013

   dx.doi.org/10.1021/ic400404g | *Inorg. Chem.* 2013, 52, 12216−12222

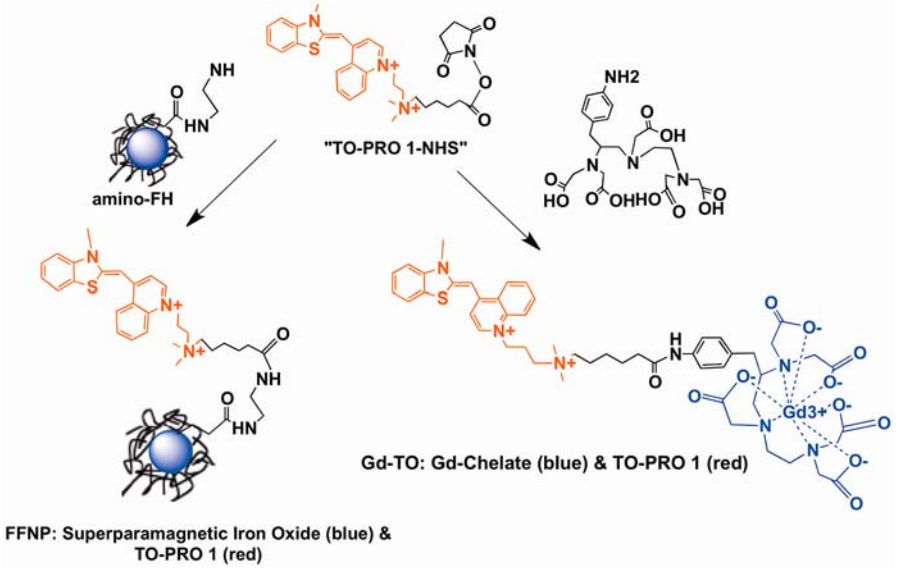

Figure 1. Syntheses of fluorochrome−metal compounds. A common intermediate is TO-PRO 1 NHS, an *N*-hydroxysuccinimide ester of TO-PRO 1. TO-PRO 1 is red. TO-PRO 1 NHS can be reacted with amino-Feraheme, an aminated version of the FH NP, to yield a FFNP. The NHS also yields Gd-TO, a DNA-binding metal chelate. FFNPs are 20−50 nm in diameter, while Gd-TO is about 1000 Da, far smaller.

DNA and Anti-DNA Antibodies in Lupus. Antibodies to DNA in the serum of patients with SLE have been studied for several decades[14,15] and more recently.[16,17] Some evidence suggests defects in DNA processing, and apoptotic cell clearance leads to the production of anti-DNA antibodies.[17−19]

DNA and Cystic Fibrosis. DNA contributes to the viscosity of mucous in cystic fibrosis, with DNase approved as a mucolytic therapy.[20−24] The origin of the DNA is host rather than microorganism.[25]

Circulating DNA. Though not a tissue biomarker for imaging, circulating DNA levels appear to be elevated in common conditions, providing another type of indication of the importance of non-nuclear DNA.[26,27] Elevated circulating levels of DNA are seen with cancer[28,29] and trauma patients.[30,31]

FFNP AND Gd-TO FEATURE INTERCALATION AS A DNA RECOGNITION MECHANISM

FFNP and Gd-TO employ the intercalating fluorochrome TO-PRO 1 for DNA recognition, in contrast to the types of interactions of many solid phases. DNA binding with silica particles is salt-mediated (Figure 2a), occurring at high ionic strength but not low ionic strength.[32−34] DNA can also form salt bridges with primary amines on many solid phases (Figure 2b).[35,36] Our approach uses TO-PRO 1 (Figure 2c), which intercalates into DNA, as shown in Figure 2d. Multiple copies of TO-PRO 1 ($n \sim 10$) are attached to a NP surface and can intercalate into double-stranded DNA, with simultaneous NP surface-to-DNA polymer interactions (Figure 2e).

FLUOROCHROME METALS THAT BIND DNA CAN HAVE A VARIETY OF VALENCIES

While Gd-TO has only one intercalating site per mole, with FFNPs n (fluorochromes per NP) can be varied between 2 and 20, with far values exceeding the $n = 2$ achieved with dimeric fluorochromes synthesized by organic chemistry.[37−40] The simultaneous interaction between multiple fluorochromes on the NP surface and multiple intercalation sites on the DNA polymer (Figure 2e) provides the basis for multivalent affinity enhancement. Because two base pairs form a site for

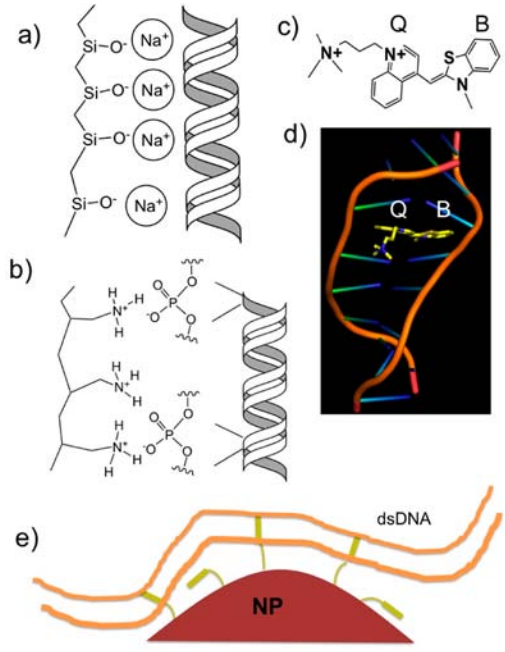

Figure 2. Electrostatic versus intercalation binding modes with DNA. (a) Ion-mediated (high ionic strength) binding of DNA and silica. (b) Salt-bridge binding between primary amines and phosphates of DNA. (c) TO-PRO 1 structure containing quinoline (Q) and benzothiazole (B) rings that intercalate into DNA. (d) Intercalation of TO-PRO 1 and double-stranded (ds)DNA. (e) FFNP featuring multiple TO-PRO 1 species (yellow) that intercalate into the dsDNA (orange). Some fluorochromes intercalate and some do not, with those failing to intercalate failing to fluoresce, as shown in Figure 4d. Base pairs are not shown.

fluorochrome intercalation,[41,42] even short sequences of DNA have large numbers of sites for intercalation. Hence, FFNPs form FFNP/DNA microaggreates when incubated with synthetic oligonucleotides was as short as 10 base pairs.[1] As Mammen et al. pointed out,[43] the affinity constants for materials with n interacting sites where each has an affinity K

dx.doi.org/10.1021/ic400404g | *Inorg. Chem.* 2013, 52, 12216−12222

are K to the nth power. Thus, the increase in the affinity achieved with multivalent FFNPs over monovalent intercalating fluorochromes is very large. Because the binding between DNA and the many fluorochromes displayed on the FFNP surface is simultaneous (Figure 2e), the transition to the unbound state requires a simultaneous breaking of multiple bonds, which is a highly improbable event.

The inability to simultaneously break multiple bonding sites generates a very low off-rate and enormous affinity between FFNPs and DNAs.

FFNPS FORM MICROAGGREGATES WHEN THEY REACT WITH DNA

Multivalent FFNPs react with DNAs from different sources to form microaggregates in solution. Microaggregate formation occurs with long DNAs (calf-thymus or phage lambda DNA) or with synthetic oligonucleotides as short as 10 base pairs. Figure 3 shows the formation of microaggregates schematically (Figure 3a) and by atomic force microscopy (AFM; calf-thymus DNA; Figure 3b,c) and dynamic light scattering (phage lambda DNA; Figure 3d). The microaggregate size is a function of the target concentration and time of reaction.

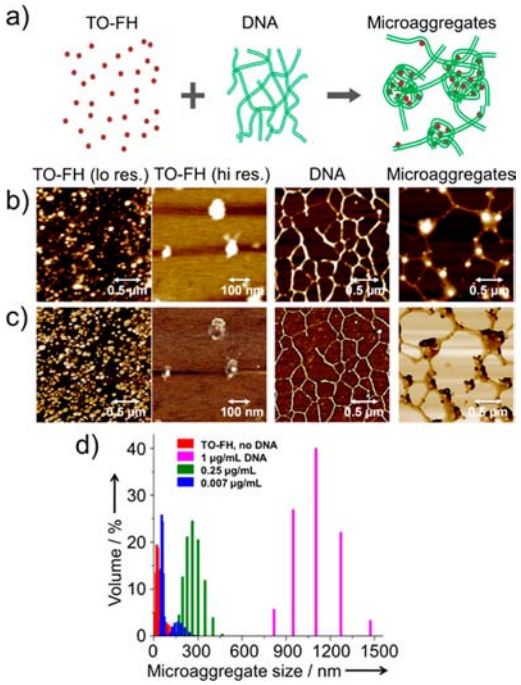

Figure 3. Formation of microaggregates when DNA reacts with a FFNP (TO-FH) by AFM or light scattering. (a) Schematic depiction of the reaction between DNA and FFNP. AFM of DNA, the FFNP, and microaggregates in topographic (b) and phase images (c). The formation of microaggregates can also be monitored, as the DNA concentration increases, by dynamic light scattering (d). Reproduced with permission from Cho and Alcantara.[2,3]

FFNP MICROAGGREGATE FORMATION IS A MORE SENSITIVE WAY TO DETECT DNA THAN FLUORESCENCE

The formation of FFNP/DNA microaggregates produced by increasing concentrations of DNA can be monitored by techniques sensitive to the fluorochrome/DNA interactions (e.g., fluorescence) or with techniques sensitive to the formation of FFNP/DNA microaggregates (e.g., T_2, light scattering), as shown in Figure 4. FFNPs with various numbers of TO-PRO 1 fluorochromes per NP (denoted as TO-FHs) were employed (Figure 4a–c), and FFNPs with approximately 10 TO-PRO 1 species per NP were selected for our studies. As shown in Figure 4c, techniques sensitive to microaggregate formation (light scattering or T_2) changed at far lower DNA concentrations than those needed for a fluorescence increase. The basis of this is shown with the schematic of Figure 4d, where the binding of a monomeric or dimeric fluorochrome to a divalent DNA is shown. When a monomeric fluorochrome binds DNA, it interacts at a single intercalating site, although there are numerous sites for intercalation on DNA. When a dimeric fluorochrome reacts with DNA (a simplification of the many fluorochromes on an FFNP), binding can occur, with some fluorochromes failing to bind and hence failing to fluoresce. (Many intercalating fluorochromes only fluoresce upon intercalation.) Because there are multivalent binding modes where binding occurs, with some fluorochromes neither intercalating nor fluorescing, DNA/FFNP microaggregate formation occurs at concentrations where fluorescence is extremely low.

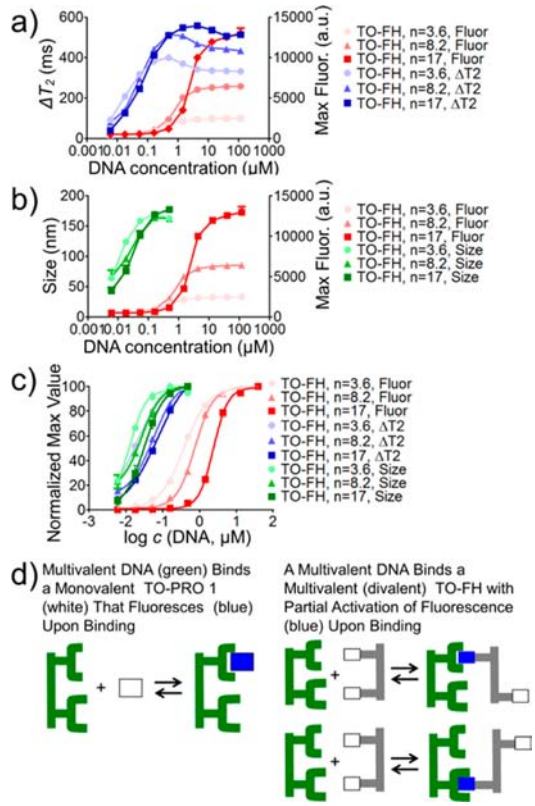

Figure 4. Reaction between FFNPs (TO-FHs) and DNA by T_2 and light scattering. These techniques measure FFNP/DNA microaggregate formation. Microaggregate response was measured by T_2 changes (a) or by light scattering (b) and compared with fluorescence. Data were analyzed by the logit equation (c). Detection by microaggregate-based techniques occurs at lower concentrations than detection by fluorescence. (d) Monovalent and divalent binding modes: the monomeric TO-PRO 1 produces its full fluorescence (blue) upon binding to DNA. A multivalent FFNP is represented as a simplified divalent fluorochrome (gray). The FFNP has DNA-binding modes that are inefficient with respect to fluorochrome activation (white-to-blue transition). Reproduced from ref 2.

dx.doi.org/10.1021/ic400404g | Inorg. Chem. 2013, 52, 12216–12222

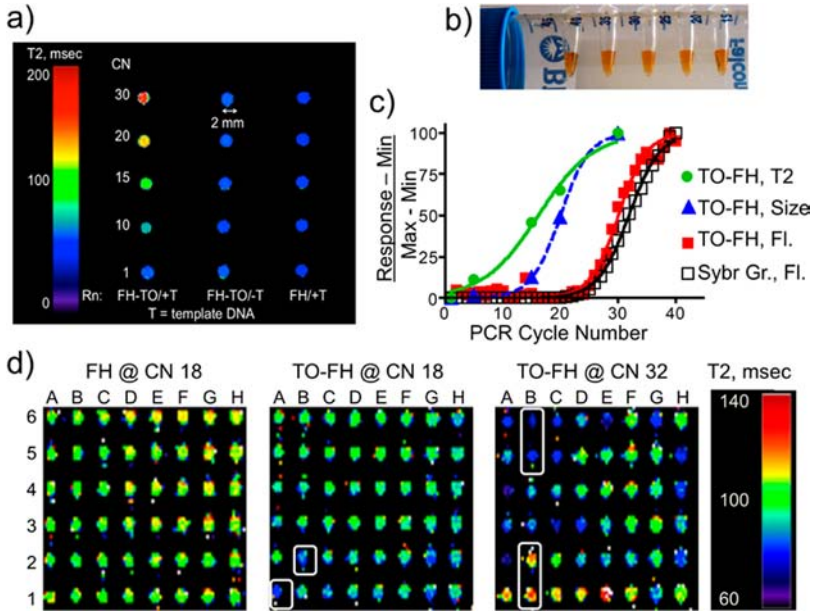

Figure 5. Monitoring PCR-generated DNA by MRI with standard PCR tubes or RT-PCR microtiter plate formats. (a) PCR reaction tubes shown in part b were imaged using a model PCR reaction at various PCR cycles (1, 10, 15, 20, and 30). With complete reagents and an FFNP (TO-FH), T_2 changed in a cycle-dependent fashion. Leaving out template DNA (T) or using a NP lacking the DNA-binding fluorochrome (FH) resulted in a constant T_2 at all cycle numbers. PCR tubes were sealed during T_2 determination, avoiding postamplification contamination. (c) Changes in T_2, microaggregate size (light scattering), or fluorescence (Fl) as a function of the PCR cycle number. Microaggregate formation, by T_2 (relaxometry at 0.47 T) or light scattering, is a more sensitive method of detecting PCR DNA than fluorescence. (d) Detection of apoptosis-related gene expression by RT-PCR using TO-FH with a microtiter plate format. Commercial microtiter plates contained different primers for apoptosis-related mRNAs, with mRNA from Jurkat cells added to all wells. Either TO-FH or FH was added to plates and PCR cycling initiated. After 18 PCR cycles, wells with TO-FH but not FH show small T_2 changes. After 32 cycles and with TO-FH, T_2 changes are greater than those at 18 cycles. TO-FH, and not FH, reacts with products of the RT-PCR reaction in a cycle-dependent fashion. MRI was at 4.7 T. Reproduced from ref 1.

FFNPS CAN MONITOR PCR-GENERATED DNA AT HIGH SENSITIVITY USING ENCLOSED REACTION TUBES THROUGH MICROAGGREGATE FORMATION

FFNPs can be added to cycling PCR tubes and the increased DNA produced by PCR cycling was detected through the formation of FFNP/DNA microaggregates (Figure 5). For an initial demonstration of this principle, we added FFNPs to cycling PCR tubes (Figure 5b) to a model PCR reaction (synthetic template and primers) and imaged closed PCR tubes as a function of the PCR cycle number (Figure 5a). In the absence of template DNA, or with a FH NP lacking TO-PRO 1, T_2 was independent of the PCR cycle number. In a separate experiment, PCR tubes were opened after the indicated cycle number and measurement of T_2 was made by relaxometry, while the size of the FFNP/DNA microaggregates was determined by light scattering (Figure 5c). Consistent with Figure 3, the detection of PCR-generated DNA by microaggregate formation, by either light scattering or T_2 changes, was more sensitive than that by fluorescence. T_2 measurements can be through sealed PCR tubes, avoiding the possibilities of post PCR amplification contamination. Because our efforts to employ FFNP were successful, we next examined whether we could monitor a commercial real-time (RT-)PCR assay run in 96-well microtiter plates (Figure 5d). RT-PCR measures the levels of a variety of mRNA levels with different primer sets that bind to different mRNA species. We therefore purchased (Qiagen) a microtiter plate containing different primer pairs in each well, with each pair designed to amplify a specific apoptosis-related mRNA. mRNAs were obtained from apoptotic Jurkat cells, cDNAs were generated, and the same cDNA mixture was added to each well of the plate. We then added our FFNP and imaged T_2 of the wells as a function of the PCR cycle number. As shown in Figure 5d, with the FFNP, T_2 changes were seen after 18 cycles, which increased in magnitude by 32 cycles. As in Figure 5a, T_2 changes did not occur with the control NP, FH, lacking a DNA binding fluorochrome. Thus, FFNPs can be used to measure PCR-generated DNA in PCR tubes or RT-PCR microtiter plate format.

By relying on multivalency-enhanced microaggregate formation, FFNPs for detecting PCR-generated DNA offer a method of detecting PCR-generated DNA at lower cycle numbers than was possible with current fluorescent techniques and may reduce amplification-related errors. In addition, the reaction of FFNPs and PCR-generated DNA can be detected from within closed PCR tubes, preventing post amplification contamination. With the development of small, hand-held relaxometers,[44−47] it is possible to envision a relaxometry-based PCR reaction run in many settings, where the fastidious technique required for current PCR technologies is replaced by more user-friendly assay formats.

FFNP OR Gd-TO CAN BE USED TO IMAGE THE DNA OF BIOLOGICAL SYSTEMS

With the interaction of FFNPs and DNA established, we next examined whether an FFNP could be used to image the DNA of biological systems. FFNPs were used to image the DNA of tumors present with an HT-29 tumor, induced to be necrotic and have permeable plasma membranes by chemotherapy (5-FU/oxaliplatin); FFNP was imaged by surface fluorescence (Figure 6a,b) or MRI (Figure 6c−f). Using the T_1-weighted

dx.doi.org/10.1021/ic400404g | Inorg. Chem. 2013, 52, 12216−12222

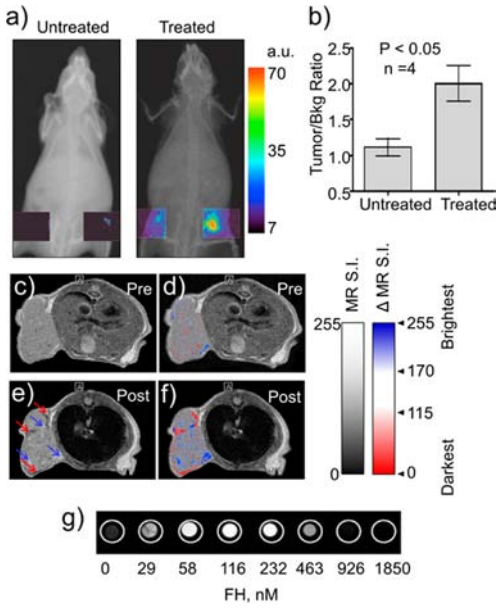

Figure 6. Imaging tumor DNA with TO-FH by surface fluorescence and MRI. Surface fluorescence is shown in parts a and b and MRI in parts c–g. (a) Tumor surface fluorescence after TO-FH injection with untreated and treated (5FU/oxaliplatin) HT-29 xenografts. (b) Tumor fluorescence, as a tumor/bkg ratio of fluorescence. (c) Pre-TO-FH MR signal intensity image. (d) Colorized version of part c with areas of highest signal intensity (brightest, blue) and lowest signal intensity (darkest, red) shown. Tumor is relatively uniform in signal intensity by MR signal intensity (c), with a few areas of high or low signal intensity shown by colorization (d). (e) Postinjection MR signal intensity image. Regions of brightening (blue arrows) and darkening (red arrows) are seen. (f) Image from part e, with areas of highest signal intensity (brightest, blue) and lowest signal intensity (darkest, red) shown. (g) Phantom image of FH solutions at varying concentrations of FH, in a nanomolar FH crystal. Using T_1-weighted pulse sequences, TO-FH can brighten or darken MR images, either of a tumor (f) or phantoms (g). Reproduced from ref 2.

pulse sequence, the uptake of FFNP brightens or darkens the tumor in a concentration-dependent manner, as shown by imaging phantoms with different NP concentrations (Figure 6g).

Our second approach to imaging DNA with fluorochrome metals employs Gd-TO, which was synthesized as shown in Figure 1. Gd-TO is used to image the DNA of necrotic Jurkat cells and the infarcted myocardium, as shown in Figure 7. Figure 7a employs phase contrast and fluorescent microscopy to show the binding of Gd-TO to Jurkat cells induced into necrotic membrane permeability by exposure to camptothecin (CPT). Gd-TO binds to the nucleus of +CPT cells, as is evident by the colocalization of Hoechst nuclear stain (blue) and Gd-TO (green). A schematic representation of part a is shown in Figure 7b. TO (blue oval) transports Gd (black circle) into the nucleus, with Gd-TO fluorescence (red) only when binding DNA.

Parts c and d of Figure 7 show Gd-TO binding to a beating mouse heart. Portions of the heart were induced into membrane-permeable necrosis by a sustained ischemia produced by vessel ligation. Gd-TO accumulated in the infarcted region, as indicated by brightening (part c), which is plotted as a T_1 map (part d). Gd-DTPA (Figure 7e,f), was not retained by the infarcted myocardium.

As shown in Figure 7g, with sustained ischemia, cells become membrane-permeable and Gd-TO binding increases (0–18 h), but thereafter DNA is cleared, leaving a non-DNA binding scar tissue. With ischemia of 100 h in duration, Gd-TO no longer binds. This enables the use of Gd-TO to distinguish acute (Gd-TO binding, new) infarctions from chronic (no Gd-TO binding, old) infarctions. Because therapeutic options can depend on the age of infarction, the ability to distinguish acute from chronic infarctions may have implications for the treatments of some organ ischemias.

■ FLUOROCHROME METALS, FUTURE PROSPECTS

Metals can be targeted to DNA *in vivo* by attaching metals (as ions or metal oxides) to DNA binding fluorochromes. Two approaches to the synthesis of fluorochrome metals are FFNPs, where the DNA binding fluorochrome TO-PRO 1 is attached to the FH iron oxide NP, and Gd-TO, where a gadolinium chelate is attached to the same DNA binding fluorochrome (Figure 1). Both types of fluorochrome metals have been used to image the DNA of necrotic cells, with FFNP employed to image the DNA of a tumor induced into necrosis by chemotherapy (Figure 6) and Gd-TO employed to image the DNA of the infarcted myocardium (Figure 7).

In addition, FFNPs form FFNP/DNA microaggregates in solution at very low DNA concentrations (Figure 3) because of multivalent interactions between the NP surface, bearing 10 fluorochromes per NP, and DNA targets possessing numerous sites for fluorochrome intercalation. FFNPs are highly stable and have been added to cycling PCR tubes and used to image PCR-generated DNA (Figure 5).

Attaching fluorochromes to the surfaces of NPs or devices provides a new and potential general way of generating nucleic acid binding surfaces. Fluorochrome-functionalized surfaces can exploit the simultaneous binding of multiple fluorochromes with multiple binding sites on DNA, a feature that leads to microaggregate formation in solution but that might be adapted to obtain magnetic particles for DNA extraction and purification in various assays and devices.

A considerable literature on fluorochrome/nucleic acid interactions exists; see, for example, ref 48, which can be mined to design fluorochromes that bind nucleic acids and that feature amine reactive *N*-hydroxysuccinimide esters for attachment to surface primary amines. Though we have employed the intercalating fluorochrome TO-PRO 1 for the development of DNA binding metals, a wide variety of fluorochromes employing a variety of binding modes (intercalation, minor or major groove binding, etc.) might be used. The recognition of nucleic acids by fluorochromes is unlikely to achieve the exquisite sequence specificity achieved with oligonucleotide hybridization. However, fluorochromes can bind certain base sequences with considerable preference,[49−51] offering prospects for the development of fluorochrome-engineered surfaces with some level of sequence selectivity.

A second type of selectivity available for fluorochrome-targeted metals is plasma membrane permeability, which can regulate the access of some fluorochromes to DNA (Figure 7b). By using the membrane-impermeable TO-PRO 1 fluorochrome, we selectively image the DNA of necrotic cells. Other membrane-impermeable DNA binding fluorochromes are propidium and Sytox Green. However, metal-ion-bearing versions of membrane-permeable, DNA-binding fluorochromes like Hoechst 33342 and DAPI, widely used as biological stains, may also be of considerable interest. Membrane-permeable

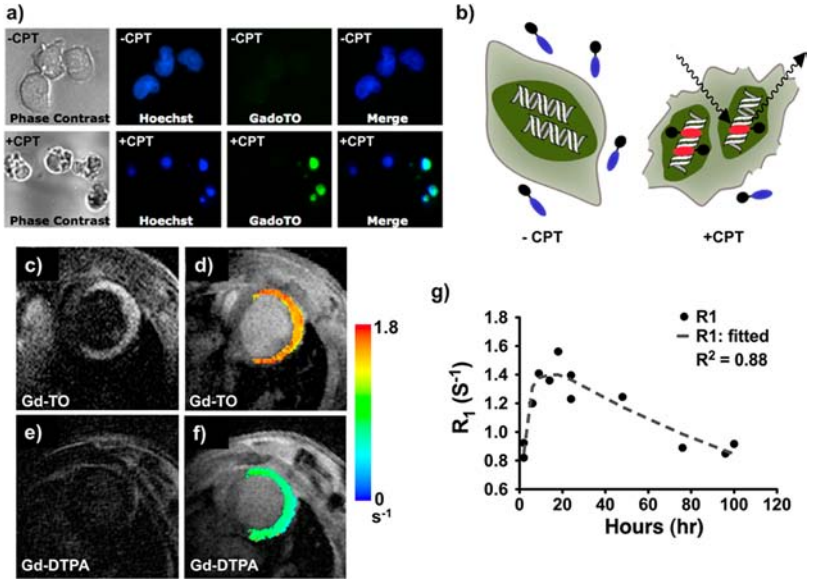

Figure 7. Gd-TO binding to the DNA necrotic Jurkat cells and to the DNA of an infarcted (necrotic) myocardium. (a) Phase contrast and fluorescence microscopy of Jurkat cells with and without treatment with CPT, which produces plasma membrane permeability. CPT induces Gd-TO (GadoTO) binding (green) that occurs in the nucleus by colocalization with a Hoechst nuclear stain (blue). b) Schematic depiction of part a. CPT induces plasma membrane breakdown. Gd-TO enters cells, binds to DNA, and fluoresces (red) upon DNA binding. Gadolinium metal (black circle) therefore binds DNA via TO (blue = nonfluorescent TO or red = fluorescent TO). Parts c–f show MRI of two beating mouse hearts induced into necrosis by a ligation/ischemia for 18 h. Mice were injected with Gd-TO (c and d) or Gd-DTPA (e and f). T_1 relaxation time in reciprocal seconds is shown on a color scale (d and f). Both mice had extensive infarcts but hearts were beating. Accumulation of Gd-TO is seen in the infarct, producing signal hyperintensity (brightening, c) and high R_1 values (d). Thus, Gd-TO (c and d) is retained in acute myocardial infarcts, while Gd-DTPA is not (e and f). (g) Dependence of Gd-TO binding to infarcted myocardium with duration of infarct. Gd-TO binding increases (0–18 h) and then declines as DNA (18–100 h) is removed. When the infarct is 100 h old, Gd-TO no longer binds. Gd-TO binding can therefore be used to tell the age of a necrotic artifact. From refs 3 and 4.

DNA-binding fluorochromes might be used to image healthy tumor cell DNA, which can be present at higher concentrations, due to mitosis, than the DNA of normal cells and tissues.

The use of DNA-binding fluorochromes to target metal oxides or metal ions to DNA may have many unexplored yet attractive applications.

AUTHOR INFORMATION

Corresponding Author

*E-mail: ljosephson@mgh.harvard.edu.

Author Contributions

The manuscript was written through the contributions of all authors. All authors have given approval to the final version of the manuscript.

Notes

The authors declare no competing financial interest.

REFERENCES

(1) Alcantara, D.; Guo, Y.; Yuan, H.; Goergen, C. J.; Chen, H. H.; Cho, H.; Sosnovik, D. E.; Josephson, L. *Angew. Chem., Int. Ed.* **2012**, *51*, 6904–6907.

(2) Cho, H.; Alcantara, D.; Yuan, H.; Sheth, R. A.; Chen, H. H.; Huang, P.; Andersson, S. B.; Sosnovik, D. E.; Mahmood, U.; Josephson, L. *ACS Nano* **2013**.

(3) Garanger, E.; Hilderbrand, S. A.; Blois, J. T.; Sosnovik, D. E.; Weissleder, R.; Josephson, L. *Chem. Commun.* **2009**, 4444–4446.

(4) Huang, S.; Chen, H. H.; Yuan, H.; Dai, G.; Schuhle, D. T.; Mekkaoui, C.; Ngoy, S.; Liao, R.; Caravan, P.; Josephson, L.; Sosnovik, D. E. *Circ.: Cardiovasc. Interventions* **2011**, *4*, 729–737.

(5) Pisetsky, D. S.; Fairhurst, A.-M. *Autoimmunity* **2007**, *40*, 281–284.

(6) Nagata, S. *Ann. N.Y. Acad. Sci.* **2010**, *1209*, 10–16.

(7) Nagata, S.; Hanayama, R.; Kawane, K. *Cell* **2010**, *140*, 619–630.

(8) Palaniyar, N.; Clark, H.; Nadesalingam, J.; Shih, M. J.; Hawgood, S.; Reid, K. B. *J. Immunol.* **2005**, *174*, 7352–7358.

(9) Palaniyar, N.; Nadesalingam, J.; Reid, K. B. *Ann. N.Y. Acad. Sci.* **2003**, *1010*, 467–470.

(10) Brill, A.; Fuchs, T. A.; Savchenko, A. S.; Thomas, G. M.; Martinod, K.; De Meyer, S. F.; Bhandari, A. A.; Wagner, D. D. *J. Thromb. Haemostasis* **2012**, *10*, 136–144.

(11) Fuchs, T. A.; Brill, A.; Duerschmied, D.; Schatzberg, D.; Monestier, M.; Myers, D. D., Jr.; Wrobleski, S. K.; Wakefield, T. W.; Hartwig, J. H.; Wagner, D. D. *Proc. Natl. Acad. Sci. U.S.A.* **2010**, *107*, 15880–15885.

(12) Brinkmann, V.; Reichard, U.; Goosmann, C.; Fauler, B.; Uhlemann, Y.; Weiss, D. S.; Weinrauch, Y.; Zychlinsky, A. *Science* **2004**, *303*, 1532–1535.

(13) Oklu, R.; Albadawi, H.; Watkins, M. T.; Monestier, M.; Sillesen, M.; Wicky, S. *J. Vasc. Interventional Radiol.* **2012**, *23*, 712–718.

(14) Ceppellini, R.; Polli, E.; Celada, F. *Proc. Soc. Exp. Biol. Med.* **1957**, *96*, 572–574.

(15) Casals, S. P.; Friou, G. J.; Myers, L. L. *Arthritis Rheum.* **1964**, *7*, 379–390.

(16) Aringer, M.; Vital, E. *Arthritis Res. Ther.* **2013**, *15*, 102.

(17) Bruner, B. F.; Guthridge, J. M.; Lu, R.; Vidal, G.; Kelly, J. A.; Robertson, J. M.; Kamen, D. L.; Gilkeson, G. S.; Neas, B. R.; Reichlin, M.; Scofield, R. H.; Harley, J. B.; James, J. A. *Arthritis Rheum.* **2012**, *64*, 3677–3686.

(18) Rahman, A.; Isenberg, D. A. *N. Engl. J. Med.* **2008**, *358*, 929–939.

(19) Olsen, N.; Li, Q.-Z.; Quan, J.; Wang, L.; Mutwally, A.; Karp, D. *Arthritis Res. Ther.* **2012**, *14*, R174.

(20) Shak, S.; Capon, D. J.; Hellmiss, R.; Marsters, S. A.; Baker, C. L. *Proc. Natl. Acad. Sci. U.S.A.* **1990**, *87*, 9188–9192.

(21) Bakker, E. M.; Tiddens, H. A. W. M. *Expert Rev. Respir. Med.* **2007**, *1*, 317–329.

(22) Ledson, M. J.; Walshaw, M. J. *Thorax* **1999**, *54*, 470.
(23) Thomson, A. H. *Cystic Fibrosis—Curr. Top.* **1996**, *3*, 289−310.
(24) Fuchs, H. J.; Borowitz, D. S.; Christiansen, D. H.; Morris, E. M.; Nash, M. L.; Ramsey, B. W.; Rosenstein, B. J.; Smith, A. L.; Wohl, M. E. *N. Engl. J. Med.* **1994**, *331*, 637−642.
(25) Lethem, M. I.; James, S. L.; Marriott, C.; Burke, J. F. *Eur. Respir. J.* **1990**, *3*, 19−23.
(26) Ziegler, A.; Zangemeister-Wittke, U.; Stahel, R. A. *Cancer Treat. Rev.* **2002**, *28*, 255−271.
(27) O'Driscoll, L. *Anticancer Res.* **2007**, *27*, 1257−1265.
(28) Fleischhacker, M.; Schmidt, B. *Nat. Med.* **2008**, *14*, 914−915.
(29) Garcia-Olmo, D. C.; Dominguez, C.; Garcia-Arranz, M.; Anker, P.; Stroun, M.; Garcia-Verdugo, J. M.; Garcia-Olmo, D. *Cancer Res.* **2010**, *70*, 560−567.
(30) Lo, Y. M.; Rainer, T. H.; Chan, L. Y.; Hjelm, N. M.; Cocks, R. A. *Clin. Chem.* **2000**, *46*, 319−323.
(31) Rainer, T. H.; Lo, Y. M.; Chan, L. Y.; Lam, N. Y.; Lit, L. C.; Cocks, R. A. *Ann. N.Y. Acad. Sci.* **2001**, *945*, 211−220.
(32) Boom, R.; Sol, C. J.; Salimans, M. M.; Jansen, C. L.; Wertheim-van Dillen, P. M.; van der Noordaa, J. *J. Clin. Microbiol.* **1990**, *28*, 495−503.
(33) Volkova, N. N.; Derjabin, O. N.; Dudchenko, N. O. *Nanosist., Nanomater., Nanotekhnol.* **2008**, *6*, 1009−1018.
(34) Marko, M. A.; Chipperfield, R.; Birnboim, H. C. *Anal. Biochem.* **1982**, *121*, 382−387.
(35) Berensmeier, S. *Appl. Microbiol. Biotechnol.* **2006**, *73*, 495−504.
(36) Bromberg, L.; Raduyk, S.; Hatton, T. A. *Anal. Chem.* **2009**, *81*, 5637−5645.
(37) Hirons, G. T.; Fawcett, J. J.; Crissman, H. A. *Cytometry* **1994**, *15*, 129−140.
(38) Gaugain, B.; Barbet, J.; Capelle, N.; Roques, B. P.; Le Pecq, J. B. *Biochemistry* **1978**, *17*, 5078−5088.
(39) Glazer, A. N.; Peck, K.; Mathies, R. A. *Proc. Natl. Acad. Sci. U.S.A.* **1990**, *87*, 3851−3855.
(40) Glazer, A. N.; Rye, H. S. *Nature* **1992**, *359*, 859−861.
(41) Benvin, A. L.; Creeger, Y.; Fisher, G. W.; Ballou, B.; Waggoner, A. S.; Armitage, B. A. *J. Am. Chem. Soc.* **2007**, *129*, 2025−2034.
(42) Persil, O.; Hud, N. V. *Trends Biotechnol.* **2007**, *25*, 433−436.
(43) Mammen, M.; Choi, S.-K.; Whitesides, G. M. *Angew. Chem., Int. Ed.* **1998**, *37*, 2754−2794.
(44) Bart, J.; Janssen, J. W.; van Bentum, P. J.; Kentgens, A. P.; Gardeniers, J. G. *J. Magn. Reson.* **2009**, *201*, 175−185.
(45) Haun, J. B.; Yoon, T. J.; Lee, H.; Weissleder, R. *Methods Mol. Biol.* **2011**, *726*, 33−49.
(46) Lee, H.; Sun, E.; Ham, D.; Weissleder, R. *Nat. Med.* **2008**, *14*, 869−874.
(47) Wensink, H.; Benito-Lopez, F.; Hermes, D. C.; Verboom, W.; Gardeniers, H. J.; Reinhoudt, D. N.; van den Berg, A. *Lab. Chip* **2005**, *5*, 280−284.
(48) Armitage, B. A. Cyanine Dye−DNA Interactions: Intercalation, Groove Binding, and Aggregation. In *DNA Binders and Related Subjects*; Waring, M. J., Chaires, J. B., Eds.; Springer: Berlin/Heidelberg, 2005; Vol. *253*, pp 55−76.
(49) Portugal, J.; Waring, M. J. *Biochim. Biophys. Acta* **1988**, *949*, 158−168.
(50) Mordy, C. W.; Carlson, D. J. *Mar. Ecol.: Prog. Ser.* **1991**, *73*, 283−293.
(51) Schnedl, W.; Breitenbach, M.; Stranzinger, G. *Hum. Genet.* **1977**, *36*, 299−305.